Optical characterization of GaAs/AlGaAs quantum well wires fabricated using arsenic implantation induced intermixing

B. S. Ooi,[a] Y. S. Tang,[b] A. Saher Helmy, A. C. Bryce, and J. H. Marsh
Department of Electronics and Electrical Engineering, University of Glasgow, Glasgow G12 8QQ, Scotland, United Kingdom

M. Paquette and J. Beauvais
Department of Electrical Engineering, University of Sherbrooke, Sherbrooke, Quebec, J1K 2R1, Canada

(Received 22 October 1997; accepted for publication 19 January 1998)

We report the fabrication of GaAs/AlGaAs quantum well wires using implantation of As at 45 keV to induce quantum well intermixing. The intermixing process was first characterized giving optimized annealing parameters of 875 °C for 30 s and an implantation dose of 1×10^{13} cm^{-2}. Wire widths from 35 to 1000 nm were defined using e-beam lithography followed by lift-off. Photoluminescence spectra from the lateral wells and barriers were observed from samples with wires as narrow as 50 nm. The energies of the lateral wells were found to remain constant for wire widths between 1000 and 150 nm, and start to shift significantly towards high energy for 80 nm wires, the signal from the lateral well eventually merging with that from the lateral barrier for 35 nm wires. An intermixing radius of about 17 nm was estimated for the process. Photoreflectance measurements were also carried out on these wire samples, showing that the wires appear to have a parabolic lateral potential and clear interwire coupling was observed from samples with barriers narrower than 50 nm. © *1998 American Institute of Physics.* [S0021-8979(98)07008-X]

I. INTRODUCTION

The optical and electronic properties of low dimension structures such as quantum well wires (QWWs) and quantum dots have attracted much interest in the past few years.[1,2] Quantum well intermixing (QWI) is one of the promising techniques for fabricating low dimensional structures, as opposed to the conventional techniques of dry etching[3] and metalorganic vapor phase epitaxy (MOVPE) selective growth on V-groove structures.[4,5] QWI can be achieved using several methods, such as impurity free vacancy induced disordering (IFVD), laser induced QWI and impurity induced disordering (IID). Although IFVD has been used to realize QWWs, lateral diffusion of vacancies generated at the surface is a limitation, and a nanometer scale resolution is therefore difficult to achieve at depths useful for guided wave optoelectronic applications.[6] Laser related induced intermixing and IID are both promising techniques to achieve nanostructure fabrication. QWWs and quantum dots have been realized by direct writing using a focused laser beam technique.[7,8] This technique involves high temperature heating induced by the laser beam to promote the interdiffusion of Al and Ga, hence locally modifying the quantum well (QW) band gap and energy level. IID can be achieved either by direct write using focused ion beams[9,10] or using other ion implantation induced disordering techniques.[11] During these techniques selected areas of a QW sample are implanted with ions to create point defects, followed by an appropriate annealing step to promote intermixing in the implanted area through diffusion of the point defects. The intermixed region has an increased band gap energy, and therefore can be used to provide lateral confinement of electrons and holes in masked unimplanted regions within the QW structure. Quantum wires prepared using this technique are buried and are therefore free of surface recombination.

Atomic mixing due to implantation in semiconductors[12] was known long before being used intentionally to induce intermixing in heterostructures.[13] For optoelectronic and photonic applications, neutral (electrically inactive) impurities are much preferred to minimize free carrier absorption.[14] For the GaAs/AlGaAs system gallium and arsenic, being the native matrix elements, have received the most attention. Gallium implantation induced intermixing has been studied,[15] and optimum annealing conditions as well as doses for broad area implantation have been deduced from experiments.[16] Also low dimensional structures have been reported for Ga implants.[17] Less progress has been achieved with arsenic implants,[11] even though arsenic has a larger mass than Ga, giving a potentially higher resolution. To the best of our knowledge, no lateral quantum confined structures have been reported previously for As implants.

In this article we report the fabrication of QWWs in a shallow single quantum well (SQW) GaAs/AlGaAs structure using As-implantation induced QWI. We first optimized the QWI process by studying the effect of QWI as a function of implantation dose, and rapid thermal annealing temperature. The quality of the material and the degrees of QWI were assessed using 77 K photoluminescence (PL) measurements. The optimum process conditions were then employed to fabricate the wire samples. Wire widths ranging between 35 and

[a]Present address: School of Electrical and Electronic Engineering, Block S1, Nanyang Technological University, Nanyang Avenue, Singapore 639798
[b]Present address: University of California-Los Angeles, Electrical Engineering Department, Los Angeles, California 90095-1594

 © 1998 American Institute of Physics

Downloaded 13 Feb 2006 to 128.100.138.249. Redistribution subject to AIP license or copyright, see http://jap.aip.org/jap/copyright.jsp

1000 nm, with a similar interwire spacing, were fabricated using e-beam lithography and a lift-off process. A 5 K PL and room temperature photoreflectance measurements were then performed on these wire samples to study the lateral potential heights and the transition states of these QWWs.

II. SAMPLE PREPARATION

Arsenic was used in this study as it is an effective intermixing species for the GaAs/AlGaAs system and electrically neutral. In addition, it has a relatively large atomic mass compared to other neutral species such as boron, fluorine and gallium, which leads to a corresponding low straggling length during ion implantation. The diffusion coefficient of As is also known to be relatively low.[18] Among the neutral species referred to above, although boron has been found to have the lowest diffusivity in GaAs/AlGaAs,[19] it is not suitable for the fabrication of QWWs as it exhibits a relatively low degree of intermixing and creates a high concentration of dislocation loops after annealing.[20] Fluorine has a high diffusivity in GaAs, and hence is expected to exhibit a large degree of lateral diffusion.

An undoped shallow single quantum well (SQW) grown by MOVPE on a GaAs substrate was used in this study. The material consisted of a 5 nm GaAs QW sandwiched between 20 and 500 nm of $Al_{0.4}Ga_{0.6}As$ barrier material above and below the well, respectively. The top barrier was covered by a 5 nm GaAs layer to prevent the $Al_{0.4}Ga_{0.6}As$ from oxidation and the bottom barrier was grown on top of a 500 nm GaAs buffer layer.

The implantation energy of As and its corresponding lateral straggling length were then simulated and optimized using TRIM, a Monte-Carlo simulation software package.[21] In order to introduce a high concentration of point defects into the QW, the peak concentration of the ion was placed at the middle of the QW. Simulation showed that 45 keV drove the ions to an average range of 27 nm, with a lateral straggle of 5 nm. Using this implantation energy, the arsenic ions will not penetrate through 50 nm of SrF_2/AlF_3, so this was used as the implant mask layer. A sharp lateral potential variation is required for the QWWs, and so one of the most important parameters is the lateral straggling length of the implanted ion. This straggling is undesirable and must be minimized. The straggling length at the depth of the QW is expected to decrease with increasing implantation energy. However, a high implantation energy will create a high degree of damage which may result in a large amount of residual damage in the QW after intermixing. Also, at high implantation energies ions will penetrate through the mask, inducing intermixing in the masked regions. The use of high energy implantation for reducing the lateral straggling was therefore not considered suitable in this study, and, to our knowledge, 45 keV is so far the lowest energy ever attempted in the fabrication of QWWs using the IID technique. Diffusion of the impurity (in this case As) and the point defects induced by the impurity and by ion implantation are other factors which influence the sharpness of the lateral potential. Due to the concentration gradient of point defects between the implanted and the masked regions, the implanted ions and defects can diffuse,

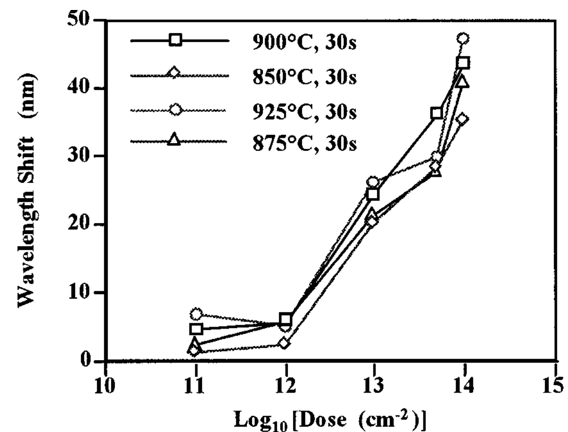

FIG. 1. Wavelength shift as a function of arsenic dose from the homogeneous implanted shallow single QW samples annealed at various RTP conditions.

and cause intermixing in the masked regions during the annealing step. The rapid thermal processing (RTP) time was, therefore, set to 30 s to minimize the lateral diffusion of impurity ions and point defects into the masked regions.

Broad area or homogeneous implantation into the shallow SQW samples was first performed to study the dose dependence of the QWI process. The as-grown samples were implanted with doses of either 1×10^{11}, 1×10^{12}, 1×10^{13}, 5×10^{13} or 1×10^{14} cm^{-2}, which correspond to peak impurity concentrations in the QW of 3.5×10^{16}, 3.5×10^{17}, 3.5×10^{18}, 1.75×10^{19}, and 3.5×10^{19} cm^{-3}. RTP was then performed at 850, 875, 900 and 925 °C for 30 s. The samples were capped with SrF_2/AlF_3 layers to prevent the out-diffusion of As during annealing. PL measurements were then carried out at 77 K to study the band gap energy shifts. Optimum dose and RTP conditions were then deduced from the quality of the PL signal and the degree of intermixing. The optimum dose and the RTP conditions found from the broad area implantation were then employed in fabricating the QWWs samples. These samples consisted of eight fields with each field containing wire masks varying from 35 to 1000 nm. The distance between the masked wires and the implanted regions was kept an equal width. The wires were defined using e-beam lithography at 100 keV, with a 20 nm spot size and 10 nm resolution. After developing, about 50 nm of SrF_2/AlF_3 were evaporated followed by lift-off in acetone to create the implantation mask. This layer was subsequently wet etched away and a fresh layer of SrF_2/AlF_3 deposited prior to annealing. Low temperature PL and room temperature photoreflectance measurements were then carried out to study the optical properties of these QWW fields.

III. MEASUREMENTS AND DISCUSSION

A. Broad area implantation

The wavelength shift as a function of As-implantation dose from the broad area implanted samples is given in Fig. 1. No apparent wavelength shift was observed from samples implanted with As doses lower than 1×10^{12} cm^{-2}, which corresponds to a peak ion concentration in the QW of about 3.5×10^{17} cm^{-3}. The impurity and point defect concentra-

Downloaded 13 Feb 2006 to 128.100.138.249. Redistribution subject to AIP license or copyright, see http://jap.aip.org/jap/copyright.jsp

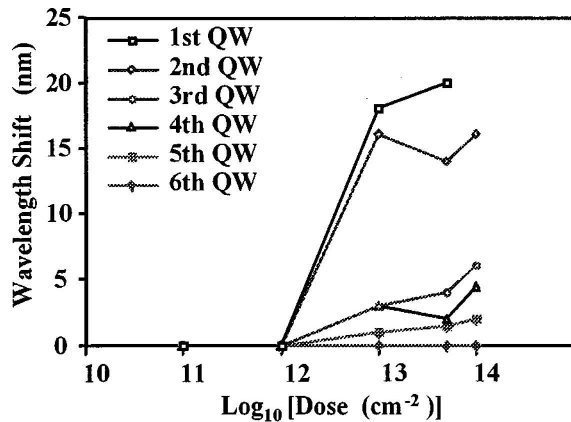

FIG. 2. The wavelength shift as a function of arsenic dose obtained from homogeneous implanted multiple-quantum well samples. The annealed conditions were 850 °C for 30 s.

tions at this dose are too low to initiate QWI. Above the threshold dose of 1×10^{12} cm^{-2}, the wavelength shift starts to increase almost linearly with increasing implantation dose. We observed no saturation in band gap shift from high implantation dose and high annealing temperature processed samples. In general, larger degrees of intermixing were observed from samples annealed at higher RTP temperatures.

Similar results were also obtained from multiple-quantum well (MQW) samples. The detailed structure of this sample has been reported elsewhere.[22] In brief, the sample consisted of six undoped GaAs QWs with well widths of 25, 36, 43, 60, 70 and 95 Å, respectively, placed 300, 525, 761, 1005, 1265, 1535 and 4535 Å below the surface. The samples were annealed at 850 °C for 30 s and the wavelength shifts, relative to control samples, i.e., unimplanted samples annealed under the same RTP conditions, are shown in Fig. 2. Only the first and the second wells showed significant band gap shifts above the critical dose of 1×10^{12} cm^{-2}, and these two QWs are located within the implantation range. From the TRIM simulation profile, the As concentration peak occurs at between 120 and 300 Å, with its tail extending as deep as 60 nm at 45 keV. With a dose of 1×10^{13} cm^{-2}, the samples had an impurity (As) concentration of about 5×10^{17} cm^{-3} at a depth of 50 nm according to the simulation profile. This concentration is above the threshold concentration of 3.5×10^{17} cm^{-3}. The degrees of intermixing decrease dramatically in the third and subsequent wells, which were situated more than 75 nm below the surface. The small degrees of intermixing observed from these wells may be attributed to the diffusion of point defects during annealing. However, ion implantation and the associated damage in GaAs/AlGaAs always appear to penetrate deeper than the theoretical predictions,[9] which may also result in the small degrees of intermixing observed from the QWs placed at 75 nm or more below the surface.

Compared to the as-grown material, the PL signals obtained from the intermixed samples, including the samples implanted with doses below the threshold dose, appeared to be broader. Weak and broad full width at half maximum (FWHM) PL signals have been detected from samples implanted with doses higher than 1×10^{13} cm^{-2}, annealed at

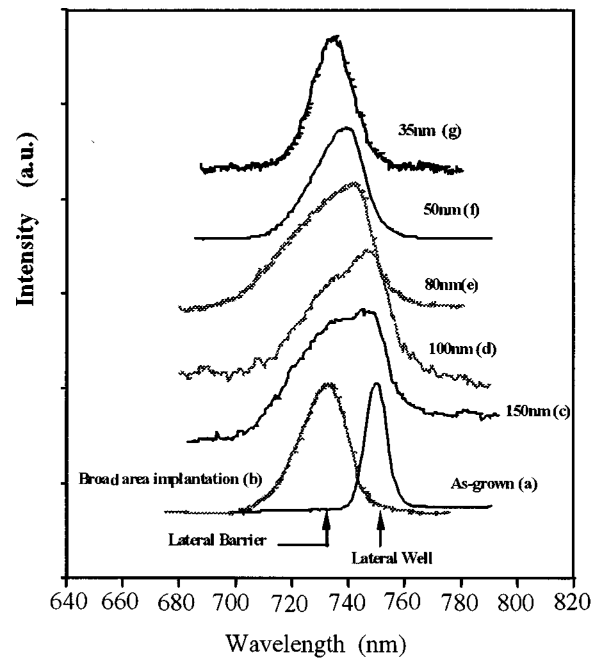

FIG. 3. Photoluminescence spectra (5 K) from (a) as-grown, (b) homogeneous implanted, and the wire samples of widths from 150 nm (c) to 35 nm (g). The samples were implanted with an arsenic dose of 1×10^{13} cm^{-2}, at 45 keV and annealed at 875 °C for 30 s.

850 °C for 30 s. This implies that the RTP temperature may be too low to activate recovery of the lattice damage. The PL signals gradually decrease in FWHM with increasing RTP temperature, becoming constant for annealing temperatures above 875 °C. The optimum RTP temperature is therefore found to be 875 °C for 30 s.

B. Photoluminescence of quantum well wires

Samples with wire widths of 1000, 500, 400, 150, 100, 80, 50, and 35 nm were implanted with 45 keV, 1×10^{13} cm^{-2} doses of As. The RTP conditions were 875 °C for 30 s. PL (5 K) measurements were performed on these samples after intermixing. Selected PL spectra are given in Fig. 3. On average, PL signals from all the intermixed samples appear to be about three times lower in intensity compared to the as-grown samples. The spectra (a) and (b) shown in Fig. 3 are the PL signals obtained from the as-grown sample and the broad area intermixed samples, respectively. The FWHM of the intermixed sample is about twice the width of the signal obtained from the as-grown sample, i.e., 20 nm for the intermixed and 9 nm for the as-grown samples. The PL from the as-grown sample peaked at 750 nm. A wavelength shift of about 17 nm (38 meV shift) was observed from the broad area implanted samples annealed under the above conditions, which is consistent with the observation of the previous experiments (Fig. 1).

The PL spectra from 1000, 500, and 400 nm wires were similar to those of the 150 nm wires [Fig. 3(c)]. We expected to observe two PL peaks from the wire samples after intermixing, one from the lateral barrier (high energy) and the other from the lateral wires (low energy). A peak at 750 nm, which is identical to the peak signal for the as-grown sample

Downloaded 13 Feb 2006 to 128.100.138.249. Redistribution subject to AIP license or copyright, see http://jap.aip.org/jap/copyright.jsp

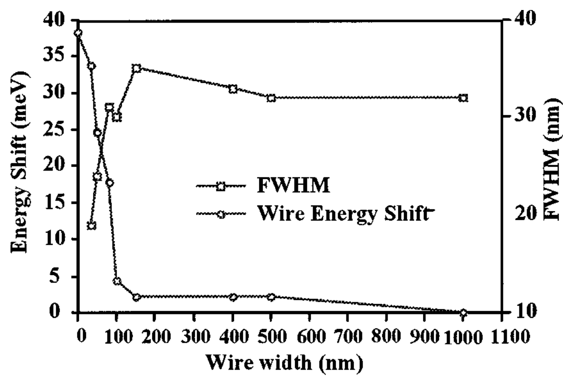

FIG. 4. The blue energy shift and the FWHM of the wire samples as function of wire width.

and a shoulder at shorter wavelength could be identified in the spectrum. The observation of the 750 nm peak from these samples confirms that the As ions did not penetrate the SrF_2/AlF_3 masks during implantation. The signals from the lateral well and from the shoulder of the lateral barrier were found to be superimposed, hence making the identification of the peak wavelength from the lateral barrier difficult. Comparing the spectrum of Fig. 3(c) to those of Figs. 3(a) and 3(b), however, we estimate that the PL peak from the lateral barrier is at about 733 nm, i.e., a lateral barrier potential of about 38 meV.

The wire emission progressively shifts towards higher energies, and decreases the FWHM, for samples with wire widths smaller than 100 nm (Fig. 4), and merges with that of the implanted barriers for 35 nm wires [Fig. 3(g)]. Although a significant wavelength shift was observed from the 50 nm wire sample, the FWHM is relatively broad compared to that of the 35 nm sample, which implies that the lateral wells are still not fully intermixed. Taking the 35 nm wires as the cutoff width for the QWI process, the intermixing radius can be estimated to be about 17 nm, which is reasonably small compared to that reported in the literature using heavy ions with higher implant energy, for example,[23] 100 nm. Compared to the lateral straggling length predicted by TRIM simulation, which is 5 nm, this result is obviously larger, implying that lateral diffusion of point defects occurs during annealing.

C. Photoreflectance of quantum well wire

The photoreflectance measurements were performed on as-grown and the wire samples at room temperature using a monochromatic tungsten-halogen lamp as the excitation source, and a 1 mW helium-neon laser mechanically chopped at 127 Hz as the modulation beam. The measured band gap for the GaAs substrate from the as-grown sample is 1.420 ± 0.001 eV. The identification of the other features in photoreflectance was done by comparing the calculated transition energies, using known structure parameters, to the measured ones. In the calculation, the effective masses of electrons, heavy and light holes were chosen to be 0.0665 m_0, 0.45 m_0 and 0.87 m_0, and a band offset split of 60/40 for the conduction/valence bands. It was found that, in addition to the band edge transitions from the substrate and the

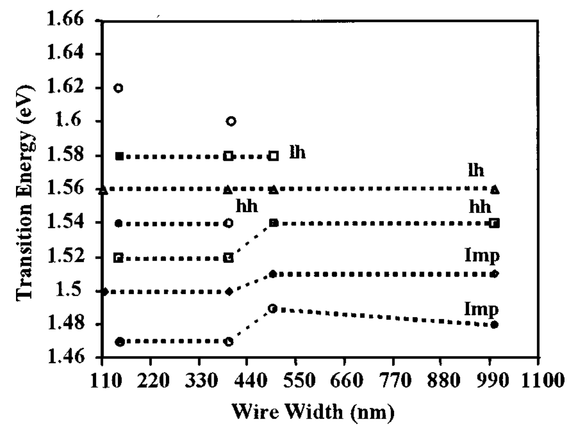

FIG. 5. Photoreflectance transitions of broad wires; notice the clear parabolic confinement potential formation starts at wire width of 500 nm. The transition energies shift down due to the transition of square well to harmonic well potential confinement.

quantum well ground state (1e-1hh) transition at 1.516 ±0.003 eV (corresponding to the 770 nm PL at 77 K), there are also transitions related to donor states in both GaAs substrate and the QW observed in the control sample. The binding energies of the impurity states for both the substrate and the QW are similar, which is 30 ± 1.5 meV. This is likely to be due to carbon contamination.

According to room temperature photoreflectance results, we can see that when the wire width is smaller than about 500 nm, the ground state transition starts to shift to red slightly, indicating that parabolic-like quantum confinement effects are starting to appear (Fig. 5). When the wires are below about 150 nm in width (Fig. 6), clear equally spaced optical transitions are observed, suggesting the confinement potentials of these wires are parabola-like, or more exactly, the potential distribution of the gratings is harmonic across the wires. Decreasing the wire width to below 100 nm induces a blueshift of the heavy hole related transitions while, at the same time, the light holes were not confined any more due to the fact that (a) a very strong inter-wire coupling

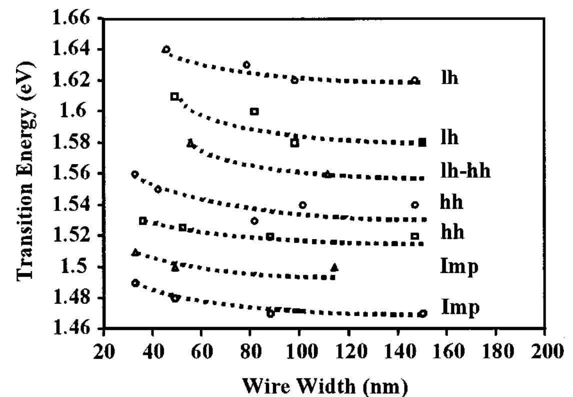

FIG. 6. Photoreflectance transitions of smaller wires; notice the equal energy separation of transitions from the heavy hole related transitions, indicating harmonic potential confinements in the wires. The relatively flat trend of light hole related transitions suggests that in wires smaller than about 100 nm, the combined effect of light effective mass for light hole and strong inter-wire coupling is so intense that light hole wave function spread everywhere across the gratings and no effective hole confinement is present.

Downloaded 13 Feb 2006 to 128.100.138.249. Redistribution subject to AIP license or copyright, see http://jap.aip.org/jap/copyright.jsp

becomes effective, and (b) the lighter effective mass of light holes lifts up the quantized states in the wells so no effective quantization is observable due to the strong inter-wire coupling effect. The harmonic potential distribution of the wire samples is expected as the wires were defined by ion implantation and the ion trajectories during As implantation create different degrees of intermixing in the QW in unmasked areas and the edges of the masked areas. This result is consistent with that obtained from the PL study. The largest wires studied here had widths of about 500 nm, with clear formation of a parabolic confinement potential in the wires occurring for a wire width of 150 nm. For the smallest (35 nm) wires, the lifting of the quantized states in the wells eliminates effective quantum confinement, although the harmonic potential variation due to ion implantation is still affecting the lifted up quantum states (or minibands), which explains the non-separable well and barrier emissions in the PL spectra.

IV. SUMMARY

We have studied and optimized the fabrication of QWWs using arsenic implantation. Shallow single GaAs/AlGaAs QW materials were implanted with doses from 1×10^{11} to 1×10^{14} cm^{-2}, with an energy of 45 keV. We observed no band gap shift for samples implanted with doses lower than 1×10^{12} cm^{-2}, which may be due to the fact that the point defect concentrations generated by these implant conditions are too low to activate the QWI process. Band gap shifts show an almost linear increase with increasing implantation dose above the threshold dose of 1×10^{12} cm^{-2}. PL measurements were performed to assess the quality and degree of the band gap shift of intermixed samples. The optimum RTP conditions were found to be 875 °C for 30 s with an arsenic dose of 1×10^{13} cm^{-2}. Similar results were also obtained from MQW samples.

QWWs with wire widths varying from 1000 to 35 nm were fabricated using e-beam lithography and a lift-off process. These samples were implanted and annealed using the optimum conditions found from the broad area implantation. We observed broad PL spectra from 1000 to 150 nm with an obvious wavelength peak at about 750 nm and a shoulder estimated to appear at about 733 nm, indicating a lateral potential height of 38 meV. These broad signals are due to the superposition of signals from the lateral wells and barriers. The lateral well shows insignificantly small shifts for wire widths between 150 and 1000 nm. Below 150 nm, the wire emission starts to show a significant blueshift and eventually merges with the lateral barrier for samples with 35 nm wires. From these results, we estimate that QWWs fabricated using this technique have an intermixing radius of about 17 nm.

Photoreflectance measurements were also performed on these samples. They confirmed those observed in the PL measurements. In addition, due to its capability of detecting higher energy transitions, photoreflectance gives us a more accurate physical picture of what is really happening in the samples in terms of each stage or degree of ion implantation induced intermixing of the quantum well in the wires. It also suggests that the combination of photoreflectance and other techniques such as PL can help us understand much better the whole process of the intermixing technique described in this article.

ACKNOWLEDGMENTS

This work was supported by the Engineering and Physical Sciences Research Council (U.K.) and by the U.K. Ministry of Defense.

[1] H. Schweizer, G. Lehr, F. Prins, G. Mayer, E. Lach, R. Krüger, E. Fröhlich, M. H. Pilkuhun, and G. W. Smith, Superlattices Microstruct. **12**, 419 (1992).
[2] D. Dragoman and M. Dragoman, IEEE J. Quantum Electron. **33**, 375 (1997).
[3] K. Kash, A. Scherer, J. M. Worlock, H. G. Craighead, and M. C. Tamargo, Appl. Phys. Lett. **49**, 1043 (1986).
[4] S. Tsukamoto, Y. Nagamune, M. Nishioka, and Y. Arakawa, J. Appl. Phys. **71**, 533 (1992).
[5] S. Tsukamoto, Y. Nagamune, M. Nishioka, and Y. Arakawa, Appl. Phys. Lett. **63**, 355 (1993).
[6] A. Pépin, C. Vieu, M. Schneider, G. Ben Assyag, R. Planel, J. Bloch, H. Launois, J. Y. Marzin, and Y. Nissim, Superlattices Microstruct. **18**, 229 (1995).
[7] K. Brunner, G. Abstrieiter, M. Walther, G. Bohm, and G. Trankle, Surf. Sci. **267**, 218 (1992).
[8] K. Brunner, U. Bockelmann, G. Abstrieiter, M. Walther, G. Bohm, G. Trankle, and G. Weimann, Phys. Rev. Lett. **69**, 3216 (1992).
[9] P. M. Petroff, Y. J. Li, Z. Xu, W. Beinstingl, S. Sasa, and K. Ensslin, J. Vac. Sci. Technol. B **9**, 3074 (1991).
[10] Y. Hirayama, S. Tarucha, Y. Suzuki, and H. Okamoto, Phys. Rev. B **37**, 2774 (1988).
[11] F. E. Prins, G. Lehr, E.M. Frohlich, H. Schweizer, and G. W. Smith, J. Appl. Phys. **73**, 2376 (1993).
[12] P. K. Haff and Z. E. Switkowski, J. Appl. Phys. **48**, 3383 (1977).
[13] J. Cilbert and P. M. Petroff, Phys. Rev. B **36**, 3243 (1987).
[14] J. H. Marsh, S. I. Hansen, A. C. Bryce, and R. M. De La Rue, Opt. Quantum Electron. **23**, S941 (1991).
[15] C. Vieu, M. Schnieder, D. Mailly, R. Planel, H. Launios, J. Y. Marzin, and B. Descouts, J. Appl. Phys. **70**, 1444 (1991).
[16] F. Laruelle, A. Bagchi, M. Tsuchiya, J. Merz, and P. M. Petroff, Appl. Phys. Lett. **56**, 1561 (1990).
[17] J. Cilbert, P. M. Petroff, D. J. Werder, S. J. Pearton, A. C. Gossard, and J. H. English, Appl. Phys. Lett. **49**, 223 (1986).
[18] Y. Hirayama, Y. Suzuki, and H. Okamoto, Jpn. J. Appl. Phys., Part 1 **24**, 1498 (1985).
[19] B. S. Ooi, A. C. Bryce, and J. H. Marsh, and J. Appl. Phys. **12**, 121 (1997).
[20] B. S. Ooi, A. C. Bryce, J. H. Marsh, and J. Martin, Appl. Phys. Lett. **65**, 85 (1994).
[21] J. F. Ziegler, J. P. Biersack, and U. Littmark, *The Stopping and Range of Ions in Solids* (Pergamon, New York, 1985).
[22] B. S. Ooi, A. C. Bryce, C. D. W. Wilkinson, and J. H. Marsh, Appl. Phys. Lett. **64**, 598 (1994).
[23] L. B. Allard, G. C. Aers, P. G. Piva, P. J. Poole, M. Buchanan, I. M. Tempelton, T. E. Jackman, S. Charbonneau, U. Akano, and I. V. Mitchell, Appl. Phys. Lett. **64**, 2412 (1994).

Downloaded 13 Feb 2006 to 128.100.138.249. Redistribution subject to AIP license or copyright, see http://jap.aip.org/jap/copyright.jsp